MODELING OF DIELECTRIC CHARGING IN RF MEMS CAPACITIVE SWITCHES

Prasad S. Sumant,[1] Andreas C. Cangellaris,[2] and Narayana R. Aluru[1]
[1] Department of Mechanical Science and Engineering, University of Illinois, 1206 W. Green St., Urbana, IL 61801; Corresponding author: psumant2@uiuc.edu
[2] Department of Electrical and Computer Engineering, University of Illinois, 1406 W. Green St., Urbana, IL 61801

Received 10 May 2007

ABSTRACT: *A unified, macroscopic, one-dimensional model is presented for the quantitative description of the process of dielectric charging in RF MEMS capacitive switches. The model provides for the direct incorporation of various physical factors known to impact dielectric charging, such as surface roughness, material inhomogeneity, and electric field-dependent conduction in the dielectric. The values of the various parameters used in the model are extracted from experimental data. The proposed model serves as a generalization of various earlier models reported in the literature for the quantitative description of dielectric charging. Its formulation is such that it can be incorporated in a straightforward manner in coupled electro-mechanical modeling schemes for the computer-aided analysis of RF MEMS capacitive switches.* © 2007 Wiley Periodicals, Inc. Microwave Opt Technol Lett 49: 3188–3192, 2007; Published online in Wiley InterScience (www.interscience.wiley.com). DOI 10.1002/mop.22903

Key words: *RF MEMS; capacitive switches; dielectric charging; surface roughness*

1. INTRODUCTION

RF MEMS capacitive switches show great potential for use in wireless communication devices [1]. However, their widespread insertion in commercial products requires further improvements in their long-term reliability. Dielectric charging is one of the factors that impact switch reliability. Dielectric charging is understood to mean the accumulation of electric charge in the insulating dielectric layer between the two electrodes of the capacitive RF MEMS switch. It can cause the switch to either remain stuck after removal of the actuation voltage or to fail to contact under application of pull-in voltage. Considerable effort has been devoted to both the experimental characterization of dielectric charging and the development of models that can be used to predict the impact of dielectric charging on electro-mechanical behavior of a capacitive switch.

First experimental characterization of dielectric charging in capacitive RF MEMS switches was demonstrated in [2]. It was qualitatively shown that switch lifetime depends exponentially on the applied voltage. This was attributed to Frenkel–Poole conduction [3], which depends exponentially on voltage. In [4] it was reported that dielectric charging was caused by charge injection. Through the experimental investigation of charging and discharging current transients a charging model was developed and used in [5] for the quantitative description of dielectric charging.

In [6] it was demonstrated that the capacitive switch lifetime is a function of the applied voltage and the contact quality between the bridge and the dielectric. In the same study it was also argued that conduction due to Frenkel–Poole emissions was responsible for charge accumulation. An experimentally fitted analytical model in [7] and a stretched exponential relaxation model in [8] are two notable models for the quantitative modeling of dielectric charging.

More recently, charge accumulation at the top and bottom interface in a capacitive switch was reported [9] for the first time. In the same work, the potential impact of surface chemistry on dielectric charging was acknowledged. Some qualitative justification was given for the observed behavior. The results reported in [9] suggest the need for further investigation into the quantitative understanding of the governing physics of dielectric charging in capacitive RF MEMS switches. For example, impact of surface roughness and material inhomogeneity in the thin-film dielectric are two of the factors that one expects to impact dielectric charging. Process induced variations and the scale of these devices make these factors all the more important. There is a need for a model that accounts for these different factors into one setting to gain more understanding about interaction of various parameters and their influence on dielectric charging.

The objective of this study is to demonstrate a one-dimensional model for the quantitative description of dielectric charging with the following attributes:

- It constitutes a generalization of the one-dimensional models reported in the literature to date;
- Utilizes experimentally-obtained data to extract parameters used for the description of the electrical properties of the model;
- Enables the calculation and monitoring of the temporal evolution of charge accumulation at the top and bottom surfaces of the insulating dielectric film;
- Enables simulation of repeated on–off operation of the switch for switch life time and reliability studies;
- Provides a means for the incorporation of the impact of the surface roughness of the electrode-dielectric interface on charge accumulation.

The study is organized as follows. We begin with the discussion of the use of an electro-quasi-static model for the physics involved in the dielectric charging during the operation of the RF MEMS capacitive switch. Next, we show how data obtained from the experimental characterization of a capacitive switch can be utilized for the assignment of appropriate values to the parameters in the electro-quasi-static model. Once these values have been assigned, the model is used for the quantitative investigation of charge accumulation for different stress voltages. We demonstrate how the proposed model provides for an easy means to perform a repeated on–off operation of the switch. Finally, we demonstrate a methodology for accounting the material surface roughness in the model.

2. PHYSICAL DESCRIPTION OF DIELECTRIC CHARGING

A generic illustration of the cross sectional geometry of a typical RF MEMS capacitive switch can be found in [9]. Despite the indicated planarity of the material interfaces, process variations during deposition result in a material surface roughness, which, in turn are responsible for a nonplanar contact between the dielectric and the two electrodes [10]. For the purpose of modeling, we assume that the metal electrodes are perfectly flat while the dielectric surface has surface asperities. This assumption simplifies modeling while imposing no restriction on the generality of the model. More specifically, as it will become apparent from the following discussion, electrode-dielectric interface roughness is macroscopically defined in terms of a very thin layer within which the electric properties (electric permittivity and conductivity) exhibit spatial variation. This is pictorially described in Figure 1. In particular, it is clearly seen from Figure 1(b) that the contact between the top electrode and the dielectric surface during the DOWN-state of the switch is not perfectly flat, leaving out air

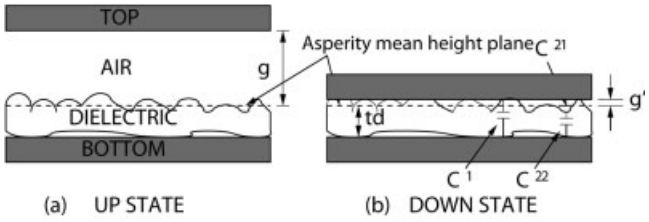

Figure 1 UP and DOWN states of a nonideal switch

pockets, resulting in the aforementioned spatial variation in the electrical properties within the layer of thickness g'. Furthermore, process variations may lead to spatial variation in the electrical properties of the dielectric. It follows immediately from Gauss' law that such spatial variations in the electric permittivity and conductivity are responsible for the accumulation of unpaired charge. Thus, a model aimed at the quantitative analysis of dielectric charging in RF MEMS switches must provide for the incorporation of such material inhomogeneities.

To provide for such a model the three-layer, piece-wise homogeneous planar structure depicted in Figure 2 is proposed. The imperfect contact at the top of the dielectric is modeled as a layer "*a*" with permittivity and conductivity different from that of the bulk dielectric. The effects of different applied voltage and changes in the quality of the contact (due to surface roughness) are captured through the use of appropriate values of the permittivity and conductivity of this layer, which are different from those in the bulk. Layer "*b*" represents the bulk of the dielectric. Finally, layer "*c*" represents the imperfect contact at the bottom side of the dielectric.

Let $V(t)$ be the impressed voltage between the two electrodes. It is assumed that the time variation is slow enough for an electro-quasi-static model to suffice for the analysis of the response of the structure to the applied voltage. Furthermore, the one-dimensional nature of the proposed model and its piece-wise homogeneous material properties imply that the electric field is constant in each one of the three layers. Let ρ_{ab} and ρ_{bc} represent, respectively, the charge densities at the top and bottom interfaces between the bulk dielectric layer and the top and bottom layers. We can then express

$$\rho_{ab} = (\varepsilon_a E_a - \varepsilon_b E_b)$$
$$\rho_{bc} = (\varepsilon_b E_b - \varepsilon_c E_c) \tag{1}$$

where ε_i, $i = a,b,c,$ denotes the electric permittivity of each layer. Application of charge conservation at each one of the two dielectric interfaces yields

$$(\sigma_a E_a - \sigma_b E_b) + \frac{\partial(\varepsilon_a E_a - \varepsilon_b E_b)}{\partial t} = 0$$
$$(\sigma_b E_b - \sigma_c E_c) + \frac{\partial(\varepsilon_b E_b - \varepsilon_c E_c)}{\partial t} = 0 \tag{2}$$

where σ_i, $i = a,b,c,$ denotes the conductivity of each layer. Finally, the equation

$$aE_a + bE_b + cE_c = V(t) \tag{3}$$

closes the system of state equations to be solved for the transient evolution of the electro-quasi-static problem.

More specifically, given $V(t)$ the system of (1)–(3) can be solved for the calculation of the electric fields in the three layers, which, in turn, through (1), can be used to obtain the temporal variation of the charge accumulation. Finally, using well-known results, the shift in actuation voltage due to charge accumulation is obtained through the equation,

$$\Delta V = \frac{h_T \rho_{ab} + h_B \rho_{bc}}{\varepsilon_b} \tag{4}$$

where h_T and h_B are, respectively, the distances of the top and bottom dielectric interfaces from the surface of the bottom electrode.

Numerical studies from the application of this model for the quantification of dielectric charging are presented in the next section. Before we proceed with these studies it is important to point out that, in its present form, the proposed model does not account for the volumetric accumulation of charge within the dielectric. However, the model can be extended to account for this contribution to dielectric charging. The way this is done will be the topic of a forthcoming study.

3. SIMULATIONS

A. Definition of Model Parameters

Experimental results reported in [9] have been used for guiding the assignment of values to the various parameters for this model. Thus, for our purposes it is assumed that the dielectric used is silicon dioxide; however, the proposed methodology is applicable to any other insulating material, provided that experimental data like those in [9] are available for the definition of the appropriate model parameters. The thickness of the dielectric layer is taken to be 0.25 μm, while its relative dielectric constant is 4.0. The top electrode is a 0.3 μm Al membrane that is grounded whereas the bottom electrode is Cr/Au. The air gap between the top electrode and the dielectric is 2.5 μm. Actuation voltage shifts (magnitude) reported for different control voltages are as follows, $\Delta V = 1.25$ V for $V = 30$ V, $\Delta V = 3.00$ V for $V = 40$ V, and $\Delta V \approx 0.0$ V for $V = 50$ V.

The values of the various parameters used in the model are presented in Table 1. For the DOWN-state (or charging or "ON " state), $a = 0.04$ μm, $b = 0.25$ μm, and $c = 0.01$ μm whereas for the UP-state (or discharging or "OFF " state), $a = 2.50$ μm (which is simply the air gap), with b and c remaining the same as expected. In view of the above, h_T, h_B are 0.26 μm and 0.01 μm, respectively.

With regards to assigning values for the conductivity in the silicon oxide, use is made of the fact that the conduction mechanism in SiO_2 is predominantly of the Fowler–Nordheim type [3],

$$J = K_1 E^2 \exp(-K_2/E) \tag{5}$$

where K_1 and K_2 are constants given by

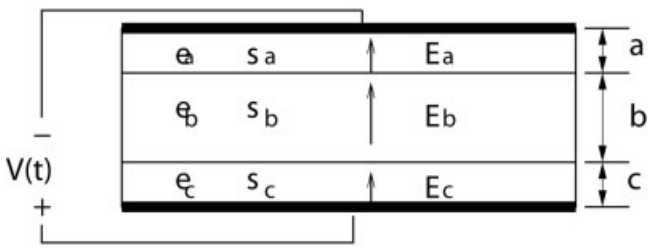

Figure 2 Three-layer model

TABLE 1 Parameters for Different Voltages

No.	Voltage (V)				(S/m)	(S/m)	(S/m)
			Charging or DOWN-state				
1	30	2.3	4.0	3.8	0.98 E −13	1.8 E −13	1.8 E −13
2	40	2.5	4.0	3.8	4.00 E −13	7.0 E −13	7.0 E −13
3	50	2.6	4.0	3.8	9.78 E −13	15.0 E −13	15.0 E −13
			Discharging or UP-state				
1	30	1.0	4.0	3.8	0.0	0.9 E −13	0.9 E −13
2	40	1.0	4.0	3.8	0.0	3.5 E −13	3.5 E −13
3	50	1.0	4.0	3.8	0.0	7.5 E −13	7.5 E −13

$$K_1 = \frac{q^3 m_o}{16\pi^2 \hbar \phi m^*} \; K_2 = \frac{4(2m^*)^{1/2}\phi^{3/2}}{3\hbar q}$$

In this equation, q is the electronic charge, $\hbar$ is the Planck's constant, m_o is the electron mass, m^* is the effective electron mass, and ϕ is the barrier potential. Thus, interpreting [5] in terms of Ohm's law with an electric field-dependent conductivity, yields the following expression for the conductivity in the dielectric

$$\sigma_b = K_1 E \exp(-K_2/E) \tag{6}$$

This expression clearly shows the exponential dependence of σ_b on the electric field in the bulk, E, and, hence, on the applied voltage V. The exact fit for bulk conductivities σ_b (Table 1) has been obtained using Eqs. (5)–(6), for barrier heights of 3.12 eV, 3.78 eV and 4.32 eV for 30 V, 40 V, and 50 V, respectively. Bulk conductivities for layers "*b*" and "*c*" during discharging (or UP-state) are taken as average of their values during charging. In the UP-state, the top layer is nothing but the air gap and hence its conductivity is taken as zero.

With regards to assigning permittivity and thickness values to the different layers, we revisit this issue in greater detail in the next section where we describe ways in which surface roughness can be incorporated in the model.

Depicted in Figure 3 is the evolution of the charge densities at the top and bottom dielectric interfaces for stress voltages of 30, 40, and 50 V. Note that the voltage is applied as a step input at t = 0, is kept at that value for 300 s and then is set to zero for the rest of the time. Also shown is the temporal evolution of the resulting actuation voltage shift. The results are in good agreement with the experimental results reported in [9]. For the case of 30 and 40 V, positive charges accumulate at both the bottom and the top interface. For the case of 50 V, a negative charge accumulates at the top interface and a positive charge at the bottom (see Fig. 3), consistent with the findings in [9]. Also, as the plot shows, the charge at the top interface has greater influence on the actuation voltage shift. Furthermore, the exponential voltage dependence of charge accumulation is evident from the plot. These results demonstrate the ability of the model to capture different physical aspects of the dielectric charging process.

B. Repeated On–Off Operation

Next we utilize the three-layer model to investigate the dielectric charging phenomenon during repeated on–off operation of the switch. More specifically, we investigate the impact of following parameters: frequency, duration and duty cycle of the actuating square wave signal. Note that, once the model parameters are defined as in section III A above, we use the same model for these studies without having to build a different model.

The switch is excited with a square wave with a peak voltage of 40 V. The simulation is carried out for two different frequencies, 10 and 100 Hz and three different duty cycles of 25% (i.e. ON for 25% of the total period, and OFF for 75% of the total period), 50 and 75%. The resulting temporal variation of the actuation voltage shifts for these cases is depicted in Figure 4. The curves for frequencies 10 and 100 Hz are very close. It is evident that frequency plays no role in dielectric charging whereas actuation voltage shift was found to increase with increasing duty cycle and duration of signal. Duty cycle determines the amount of time

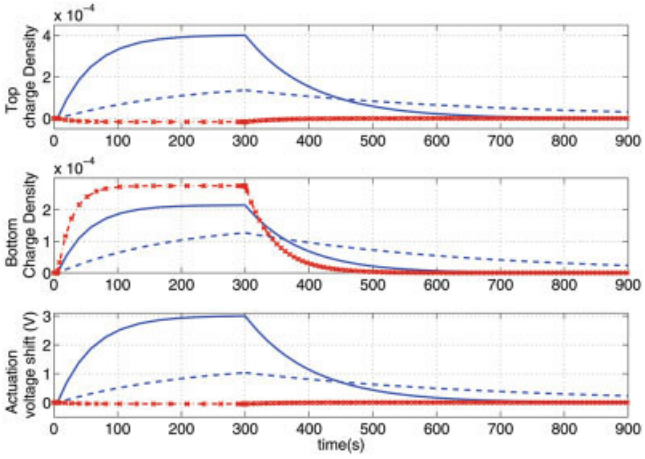

Figure 3 Charge densities and actuation voltage shift as a function of control voltage: 30 V (blue dash line), 40 V (blue solid line) and 50 V (red line with "x"). [Color figure can be viewed in the online issue, which is available at www.interscience.wiley.com]

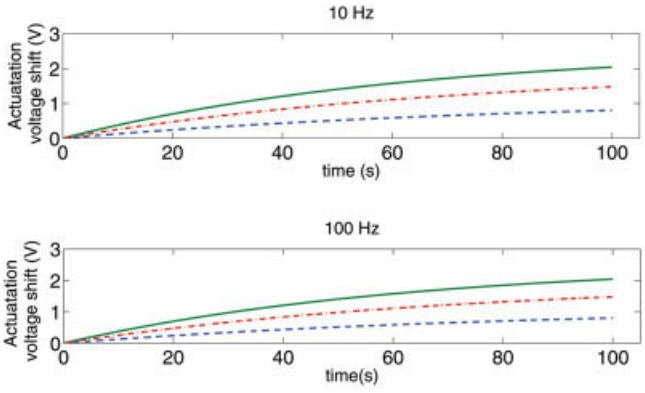

Figure 4 Actuation voltage shift as a function of frequency, duty factor and time, 40 V square wave signal. "Solid line": 75% "dash dot line": 50% "dashed line": 25%. [Color figure can be viewed in the online issue, which is available at www.interscience.wiley.com]

available for charging in a given time period. As the duty cycle is increased from 25 to 75%, the amount of time available for charging increases thus resulting in greater charge accumulation and hence greater actuation voltage shifts. All these results are consistent with the experimental findings reported in the literature [11].

As already mentioned in the introduction, the parameters chosen for the definition of the proposed three-layer model have been motivated by the desire to provide means for incorporating in the model several of the physical effects that govern dielectric charging. For example, it will be demonstrated in the following section that the variation of the permittivity of the top contact layer with voltage can be related to the surface roughness of the dielectric surface. The same also holds for the thickness of the layers. Furthermore, as demonstrated through the example in this section, allowing the bulk conductivity to be voltage dependent provides for incorporating in the model the appropriate conduction mechanism for the insulating material under consideration.

4. IMPACT OF SURFACE ROUGHNESS

Surface roughness plays an important role in the quality of the electrical contact between the metal electrode and the insulating dielectric. More specifically, it dictates the effective (actual) contact area at the metal-dielectric interface [10]. In what follows, we employ the Greenwood–Williamson (GW) model [12] used in [10] to demonstrate how the impact of surface roughness can be incorporated in the model. Without loss of generality, our presentation assumes roughness at the top dielectric interface. Roughness at the interface between the dielectric and the bottom electrode can be handled in the same manner.

The GW model utilizes the following three parameters: (a) the assumed constant radius, R, of the spherical asperities; (b) the standard deviation, σ_s, of the asperity height, assumed to be a Gaussian distribution; (c) the asperity density, D_{SUM}. These parameters can be extracted from experimental measurements of moments of surface topography [10].

Let us consider the DOWN-state of the switch (see Fig. 1). On the basis of the GW model, the actual contact area with respect to apparent contact area A_0 is given by [10],

$$A^* = \frac{A_c}{A_0} = 0.064(\alpha - 0.8968)^{1/2} \int_{g'}^{\infty} \left(\frac{z - g'}{g'}\right) \phi(z)dz \quad (7)$$

where A_c is the real contact area and g' is the separation between the top electrode and the asperity-mean-height plane. As the top electrode approaches the dielectric layer, g' will decrease. The separation g' is related to the applied load. The load P on the switch is a combination of the electrostatic force of attraction and the restoring elastic force,

$$P = F_{elect} - F_{elast}$$
$$F_{elect} = \frac{1}{2} C^r \frac{V^2}{t_d} \quad F_{elast} = k(g - t_d - g') \quad (8)$$

In the above equations, C^r denotes the real DOWN-state capacitance, k is the effective spring constant, t_d is the thickness of the dielectric layer, and V is the applied voltage. The real DOWN-state capacitance can be expressed as

$$C^r = C^1 + C^2 \quad (9)$$

where C^1, C^2 are, respectively, the capacitances corresponding to surface areas where the top electrode contacts and does not contact the dielectric surface. C^2 can be further split into two parts, C^{21} and C^{22}, which come from the air gap between the metal bridge and the silicon dioxide and the silicon dioxide itself, respectively, as illustrated in Figure 1(b). Thus, we have,

$$C^1 = \frac{\varepsilon_0 \varepsilon_r A_0 A_r}{t_d + g'} \quad (10)$$
$$\frac{1}{C^2} = \frac{1}{C^{21}} + \frac{1}{C^{22}}$$
$$\frac{1}{C^{21}} = \frac{\varepsilon_0 A_0 (1 - A^*)}{g'}, \frac{1}{C^{22}} = \frac{\varepsilon_0 \varepsilon_r A_0 (1 - A^*)}{t_d}$$

In addition, we define the normalized DOWN-state capacitance as

$$C^* = \frac{C^r}{C^a} \quad (11)$$

where C^a is the capacitance corresponding to the apparent contact area A_0.

Equations (7)–(11) form a set of nonlinear equations in g', which can be solved iteratively to obtain a value of g' and, hence, C^*, for different applied voltages. A detailed set of equations can be found in [10, 12] and will not be repeated here.

Next, we compute the voltage dependence of the normalized, DOWN-state capacitance for the following roughness parameters $\sigma_s = 6.8$ nm, $R = 18.23$ nm, $D_{SUM} = 509\ \mu\mathrm{m}^{-2}$, and material properties, $E_{A1} = 70$ GPa, $\nu_{A1} = 0.34$ and $E_{SiO_2} = 75$ GPa, $\nu_{A1} = 0.20$ [13]. We also compute the voltage dependence of the normalized, DOWN-state capacitance from the series connection of the capacitances of the layers in the three-layer model developed in section II. This comparison is depicted in Figure 5. The comparison demonstrates consistency between the two approaches. This means that we can use DOWN-state capacitance calculated using surface roughness data [Eq. (10) above] and compute an effective permittivity ε_a for the top layer. Furthermore, the thickness a of the top layer in the three-layer model (section III) is approximately $6\sigma_s$. This implies that the top layer can be considered to be of thickness encompassing >99% of surface asperities.

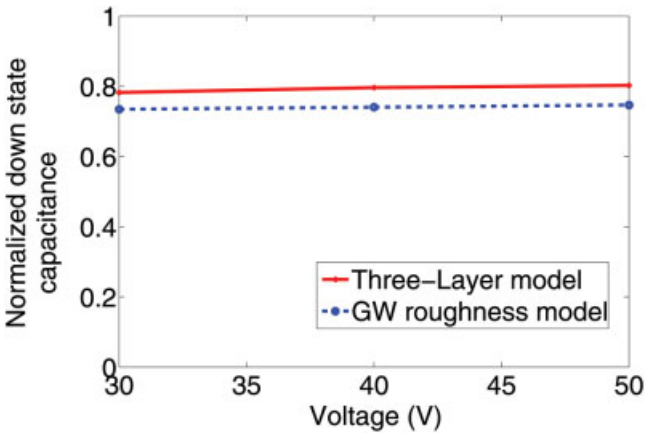

Figure 5 Comparison of DOWN-state capacitance from GW roughness model and three-layer model. [Color figure can be viewed in the online issue, which is available at www.interscience.wiley.com]

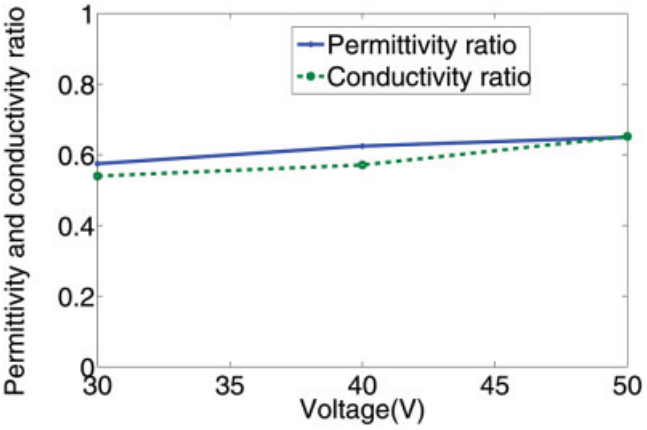

Figure 6 Voltage variation of permittivity and conductivity of top layer as a fraction of bulk properties. [Color figure can be viewed in the online issue, which is available at www.interscience.wiley.com]

Next, we plot the variation of permittivity and conductivity of top layer "*a*" as a fraction of bulk properties "*b*" in Figure 6. These results clearly demonstrate a strong correlation between surface roughness and effective permittivity, conductivity and thickness of the top contact layer in the three-layer model.

5. CONCLUDING REMARKS

In summary, we have presented a one-dimensional, electro-quasi-static model for the macroscopic, quantitative description of the process of dielectric charging in RF MEMS capacitive switches. The proposed model provides for a unifying framework for the incorporation of several of physical attributes and processes known to impact dielectric charging. More specifically, the model allows for the specific conduction mechanism in the dielectric to be taken into account in the model. In addition, it provides for the impact of the imperfect contact at the metal-dielectric interface, which is due to surface roughness, to be incorporated in the model. The proposed model relies on experimental input for the definition of several of the parameters used. More specifically, the model parameters can be extracted through experiments involving surface roughness characterization and capacitance and conductivity measurements as a function of applied voltage.

ACKNOWLEDGMENT

This research was supported by the Defense Advance Research Programs Agency (DARPA) under Grant HR0011-06-1-0046.

REFERENCES

1. H.A.C. Tillmans, W.D. Raedt, and E. Beyne, MEMS for wireless communications: From RF-MEMS components to RF-MEMS-SIP, J Micromech Microeng 13 (2003), S139–S163.
2. C. Goldsmith, J. Ehmke, A. Malczewski, B. Pillans, S. Eshelman, Z. Yao, J. Brank, and M. Eberly, Lifetime characterization of capacitive RF MEMS switches, IEEE MTT-S Int Microwave Symp Dig, Phoenix, AZ (2001), 227-230.
3. S.M. Sze, Physics of semiconductor devices, Wiley, New York, 1969.
4. X. Yuan, S.V. Cherepko, J.C.M. Hwang, C.L. Goldsmith, C. Nordquist, and C. Dyck, Initial observation and analysis of dielectric charging effects on RF MEMS capacitive switches, IEEE MTT-S Int Microwave Symp Dig, Forth Worth, TX (2004), 1943-1946.
5. X. Yuan, J.C.M. Hwang, D. Forehand, and C.L. Goldsmith, Modeling and characterization of dielectric charging effects in RF MEMS capacitive switches, IEEE MTT-S Int Microwave Symp Dig, Long Beach, CA (2005), 753-756.
6. S. Melle, D.D. Conto, D. Dubuc, K. Grenier, O. Vendier, J.-L. Muraro, J.-L. Cazaux, and R. Plana, Reliability modeling of capacitive RF MEMS, IEEE Trans Microwave Theory Tech 53 (2005), 3482-3488.
7. W.M.v. Spengen, R. Peurs, R. Mertens, and I.D. Wolf, A comprehensive model to predict the charging and reliability of capacitive RF MRMS switches, J Micromech Microeng 14 (2004), 514-521.
8. G.J. Papaionnou, M. Exarchos, V. Theonas, G. Wang, and J. Papapolymerou, On the dielectric polarization effects in capacitive RF MEMS switches, IEEE MTT-S Int Microwave Symp Dig, Long Beach, CA (2005), 761-764.
9. Z. Peng, X. Yuan, J.C.M. Hwang, D. Forehand, and C.L. Goldsmith, Top vs. bottom charging of the dielectric in RF MEMS capacitive switches, Proceedings of Asia-Pacific Microwave Conference, Yokohoma, Japan (2006).
10. A.B. Yu, A.Q. Liu, Q.X. Zhang, and H.M. Hosseini, Effects of surface roughness on electromagnetic characteristics of capacitive switches, J Micromech Microeng 16 (2006), 2157-2166.
11. X. Yuan, Z. Peng, J.C.M. Hwang, D. Forehand, and C.L. Goldsmith, A transient SPICE model for dielectric-charging effects in RF MEMS capacitive switches, IEEE Trans Electron Dev 53 (2006), 2640-2648.
12. J.I. McCool, Comparison of models for the contact of rough surfaces, Wear 107 (1986), 37-60.
13. G.M. Rebeiz, Rf MEMS theory, design, and technology, Wiley, New Jersey, 2003.

ERRATUM: DUAL AND TRIPLE-BAND PIFA DESIGN FOR WLAN APPLICATIONS

Chow-Yen-Desmond Sim
Department of Computer and Communication Engineering, Chienkuo Technology University, Chang-Hua City, Taiwan 500, Republic of China; Corresponding author: cyds@ctu.edu.tw

Received 5 February 2007

ABSTRACT: *Originally published Microwave Opt Technol Lett 49: 2159–2162, 2007.* © 2007 Wiley Periodicals, Inc. Microwave Opt Technol Lett 49: 3192, 2007; Published online in Wiley InterScience (www.interscience.wiley.com). DOI 10.1002/mop.22885

It has been brought to our attention that Table 1 was missing vertical arrows, which are vital to the readers regarding the parametric results of the author's research. Table 1 should appear as follows:

We apologize for any inconvenience this error may have caused.

TABLE 1 Trends of Both Resonant Frequencies and Their Respective Input Impedance as a Function of the Geometrical Parameters of the Proposed Dual-Band PIFA 1

Parameters	f_L	f_H	SWR_L	SWR_H
A ↑	↓	SV	SV	SV
B ↑	↓	SV	↓	↓
C ↑	SV	↓	SV	SV
D ↑	↑	↑	SV	↑
Lg ↑	SV	SV	↓	SV
Wg ↑	SV	SV	↓	↓
Lp ↑	↓	↓	↓	↑
Wp ↑	↓	↓	↑	↓
Ls ↑	↑	SV	↓	SV
h ↑	↓	↓	↑	↓